

# **Age of Donor of Human Mesenchymal Stem Cells Affects Structural and Functional Recovery after Cell Therapy Following Ischaemic Stroke**

Susumu Yamaguchi, MD; Nobutaka Horie, MD, PhD; Katsuya Satoh, MD, PhD;  
Takeshi Ishikawa, PhD; Tsuyoshi Mori, PhD; Hajime Maeda, MD; Yuhtaka Fukuda,  
MD; Shunsuke Ishizaka, MD, PhD; Takeshi Hiu, MD, PhD; Yoichi Morofuji, MD,  
PhD; Tsuyoshi Izumo, MD, PhD; Noriyuki Nishida, MD, PhD; Takayuki Matsuo, MD,  
PhD

Department of Neurosurgery (S. Y., N. H., H. M, Y. F, S. I., T. H., Y. M., T. I., T. M.),  
and Department of Molecular Microbiology and Immunology (K. S., T. I., T. M., N.  
N.), Graduate School of Biomedical Sciences, Nagasaki University, Nagasaki, Japan

**Address correspondence and reprint requests to:** Nobutaka Horie, MD, PhD,

Department of Neurosurgery, Graduate School of Biomedical Sciences, Nagasaki

University, 1-7-1, Sakamoto, Nagasaki 852-8501, Japan. Tel.: 81-095-819-7375, FAX:

81-095-819-7378, E-mail: [nobstanford@gmail.com](mailto:nobstanford@gmail.com)

## **Sources of funding**

This work was supported in part by a grant-in-aid for Scientific Research to Dr Yamaguchi

(#26861155) and Dr Horie (#26462165).

**Running headline:** Donor Age and Cell Transplantation After Stroke

**Figure: 7, Table: 0, Supplemental File: 1**

***Abstract***

Cell transplantation therapy offers great potential to improve impairments after stroke. However, the importance of donor age on therapeutic efficacy is unclear. We investigated the regenerative capacity of transplanted cells focusing on donor age (young v. old) for ischaemic stroke. The quantities of human mesenchymal stem cell (hMSC)-secreted brain-derived neurotrophic factor *in vitro* and of monocyte chemoattractant protein-1 at day 7 *in vivo* were both significantly higher for young hMSC compared with old hMSC. Male Sprague-Dawley rats subjected to transient middle cerebral artery occlusion that received young hMSC (trans-arterially at 24 h after stroke) showed better behavioural recovery with prevention of brain atrophy compared with rats that received old hMSC. Histological analysis of the peri-infarct cortex showed that rats treated with young hMSC had significantly fewer microglia and more vessels covered with pericytes. Interestingly, migration of neural stem/progenitor cells expressing Musashi-1 positively correlated with astrocyte process alignment, which was more pronounced for young hMSC. Aging of hMSC may be a critical factor that affects cell therapy outcomes, and transplantation of young hMSC appears to provide better functional recovery through anti-inflammatory effects, vessel maturation, and neurogenesis potentially by the dominance of trophic factor secretion.

**Keywords:** aging, cell transplantation, neuronal-glia interaction, stroke, stem cell

## **Introduction**

Recent advances in stroke treatment including antithrombotic drugs and endovascular techniques have provided better outcomes.<sup>1</sup> Nevertheless, post-stroke treatment is still challenging for patients suffering stroke-induced motor weakness, speech disturbances, and other deficits, which directly affect their daily activity and quality of life. Cell transplantation therapy holds great promise for such impairments after stroke,<sup>2</sup> and many clinical trials are currently ongoing worldwide.<sup>3</sup> This new strategy, however, has some fundamental questions that remain to be answered including adequate candidate donors (age, aetiology, infarct size, and lesion), best donor cell-type, optimal cell dose, timing, and delivery route.<sup>4-6</sup>

Mesenchymal stem cells (MSCs) are an attractive source of cells for transplantation after stroke as they are relatively easy to obtain and culture. While MSCs can transdifferentiate into endothelial or neural cells, it was shown they have a restorative effect by aiding injured brain and enhancing endogenous recovery after stroke.<sup>6</sup> Autologous transplantation has minimal safety concerns because a patient's own MSCs can be used for therapy. We previously reported that the intra-arterial MSC transplantation of adult

human cells improved experimental stroke models both functionally and histologically.<sup>4</sup>

<sup>6</sup> However, the age of the MSC donor may affect stem cell functions.<sup>7</sup> Older MSCs were reported to have decreased proliferation and secretion of trophic factors.<sup>8</sup> In cell transplantation for cardiovascular or other diseases, stem cells from older people were reported to have decreased regenerative capacities.<sup>9-13</sup> We assume that these unfavourable characteristics of aged stem cells might also affect the success of cell therapy for stroke.

High levels of serum brain-derived neurotrophic factor (BDNF) were reported to provide good functional recovery after ischaemic stroke<sup>14</sup>, and BDNF secreted from MSC was an important neurotrophic factor in cell transplantation therapy following ischaemic stroke.<sup>15</sup> A recent clinical study also suggested that higher levels of platelet-derived growth factor (PDGF)-BB produced from MSC<sup>16, 17</sup> were associated with better functional outcomes after intra-arterial transplantation for stroke.<sup>18</sup> Therefore, we investigated (1) whether the level of BDNF and PDGF-BB secretion differs between young and old human MSCs (hMSCs), and (2) whether donor age affects functional and structural recovery in addition to inflammation, neovascularisation and endogenous neural stem/progenitor cell migration. Finally, we assessed the hypothesis that hMSCs from younger donors provide better recovery with structural arrangement after transplantation for ischaemic stroke.

## **Materials and methods**

### **Ethics statement**

All animal experiments were conducted according to the Guidelines for Proper Conduct of Animal Experiments by the Science Council of Japan (1 June 2006) (<http://www.scj.go.jp/ja/info/kohyo/pdf/kohyo-20-k16-2e.pdf>). All animal procedures were performed in accordance with and approved by the Administrative Panel on Laboratory Animal Care of Nagasaki University and in accordance with the ARRIVE guidelines.

### **Animals**

We used 86 male Sprague-Dawley rats (aged 8–9 weeks, weighing 250–330 g). Rats were housed three per cage in the animal facility of Nagasaki University at  $24\pm 3$  °C and  $60\pm 25\%$  humidity with 12 h of light per day and with free access to food and water. The animals were allocated to experimental groups randomly using a manual method (ghost leg). Sample size was determined as previously described.<sup>4,6</sup>

### **Trophic Factor Quantification and Proliferative Activity of hMSC *In Vitro***

The levels of trophic factors were measured from two hMSC groups: young hMSCs from RIKEN BRC (Tsukuba, Japan), Lonza (Tokyo, Japan), Cosmo Bio (Tokyo, Japan),

and old hMSCs from RIKEN BRC, Takara Bio (Kusatsu, Japan). Levels of BDNF (young hMSCs: n=5, 20–34 years, median 25.0 years; old hMSCs: n=6, 57–77 years, median 63.5 years), and PDGF-BB (young hMSCs: n=3, 20–30 years, median 25 years; old hMSCs: n=4, 57–65 years, median 61.5 years) were quantified *in vitro*. Cells were plated into a 6-well dish ( $1 \times 10^5$  cells, n1) and cultured in MSCGM™ (Lonza, Japan; Product Code: PT-3001). At confluence, cells were made quiescent by incubation in 1 ml of medium containing basic fibroblast growth factor (10 ng/ml). Twenty-four hours later, supernatants were collected and cell numbers (n2) were counted. Conditioned medium (CM) was analysed by Luminex assay. A MILLIPLEX MAP kit (Millipore, Bedford, MA, USA) was used for microsphere-based multiplex immunoassays to measure the concentrations of BDNF and PDGF-BB.

Doubling time was calculated at passage, using the following formula: doubling time (days) = culture time (days)  $\times \ln(2) / \ln(n2/n1)$ .

### **Middle Cerebral Artery Occlusion and Reperfusion Model**

Transient middle cerebral artery occlusion was performed for 75 min with 4.0 nylon monofilament sutures coated with silicone (4039PK10; Docol) as previously described.<sup>4,</sup>

<sup>6, 19</sup> Rats showing a modified neurological severity score (mNSS) from 6 to 9 points at 24 h post-stroke were included in this study.<sup>20</sup>

## Cell Culture and Transplantation

hMSCs obtained from RIKEN BRC were originally isolated by iliac crest aspiration from a 64-year-old man and a 24-year-old man.<sup>21</sup> As previously described, cells were prepared and cells or phosphate buffered saline (PBS) were injected into the internal carotid artery through a catheter inserted from the stump of the distal external carotid artery to the internal carotid artery via bifurcation at 24 h after cerebral infarction.<sup>4</sup> Nutrition and hydration for all animals were provided in accordance with the Administrative Panel on Laboratory Animal Care of Nagasaki University. Rats with severe stroke were housed in separate cages to allow easy access to food and water.

We divided the animals into three groups: young hMSC group (24-year-old MSCs  $1 \times 10^6$  cells/300  $\mu$ l); old hMSC group (64-year-old MSCs  $1 \times 10^6$  cells/300  $\mu$ l); and control group (PBS 300  $\mu$ l). The operator was blinded to the age and treatment group allocation during surgery. Cell dose ( $1 \times 10^6$ ) was determined based on previous reports including our own.<sup>4, 6, 22</sup> Cyclosporine A (10 mg/kg) was injected intraperitoneally once every 2 days until euthanasia. The number of rats used for each experiment is summarised in Supplementary Table 1. The following conditions excluded rats from analyses: (1) ineligible mNSS outside 6 to 9 points (n=16), (2) death (control group (n=5), old hMSC group (n=5), young hMSC group (n=4)), and (3) postoperative complication (n=1). Experiments were



reported according to the ARRIVE guidelines.

### **Neurobehavioural Assessment**

To evaluate the functional recovery of rats (young hMSC group; n=9, old hMSC group; n=8, control group; n=10), behavioural assessment was performed at days (D)0, 1, 2, 7, 10, 14, 17, and 21 after stroke using the mNSS, which consisted of motor, sensory reflex and balance tests (Supplementary Table 2). Investigators were blinded to treatment group allocation during outcome evaluation.

### **Tissue Processing and Immunohistochemistry**

After deep anaesthesia using isoflurane, we performed perfusion fixation using 100 ml 4% paraformaldehyde (PFA) after 100 ml of cold saline via the ascending aorta at D2, D7, or D21. Then, brains were removed and postfixed in 4% PFA overnight and equilibrated in 30% sucrose at 4 °C. After brains sank in the solution, 40- $\mu$ m frozen coronal sections were prepared. All sections for immunofluorescence staining were stained by the free-floating method. For immunofluorescence staining, sections were incubated with primary antibodies (mouse anti-RECA-1: Abcam, Tokyo, Japan; 1:500, rabbit anti-Iba-1: Wako Chemicals, Osaka, Japan; 1:500, mouse anti-gial fibrillary acidic protein (GFAP): MAB3402; Chemicon, Temecula, CA, USA; 1:500, rat anti-Musashi-1 (Msi-1): Medical and Biological Laboratories Co. Ltd, Nagoya, Japan; 1:100) overnight

at 4 °C or other primary antibodies (mouse anti-human cytoplasmic marker STEM 121:AB-121-U-050; Stem Cells Inc., Palo Alto, CA, USA; 1:100, rabbit anti-platelet-derived growth factor receptor (PDGFR)- $\beta$ : Cell Signaling Technology Inc., Danvers, MA, USA; 1:50) for two nights at 4 °C. They were then incubated with secondary antibodies (TOPRO-3: Molecular Probes, 1:1000; Alexa Fluor 488 goat anti-mouse IgG: Molecular Probes, 1:1000; Alexa Fluor 488 goat anti-rabbit IgG: Molecular Probes, 1:1000; Alexa Fluor 488 goat anti-rat IgG: Molecular Probes, 1:1000; Alexa Fluor 594 rabbit anti-mouse IgG: Molecular Probes, 1:500; Alexa Fluor 594 donkey anti-mouse IgG: Molecular Probes, 1:500; Alexa Fluor 594 rabbit anti-rat IgG: Molecular Probes, 1:500) for 2 h at room temperature. The sections were analysed using a confocal laser microscope (LSM5 Pascal Ver3.2; Zeiss).

### **Immunohistochemical Analyses**

All quantifications and analyses were performed by an examiner blinded to treatment allocation. At both D2 and D7, four rats in each group were analysed by immunohistochemistry. At D21, nine rats in the young hMSC group, eight rats in the old hMSC group and ten rats in the control group were analysed by immunohistochemistry. Two regions (450 $\times$ 450  $\mu$ m per region) of interest in the peri-infarct cortex per section of three sections were analysed from each rat. The number of transplanted hMSCs was

measured by counting STEM 121 and TOPRO-3 double-positive cells at D2, D7, and D21. The areas of RECA-1–positive vessels and Iba-1–positive microglia were measured using WinRoof software (Mitani Corporation; Tokyo, Japan) at D21. The number of vessels covered by pericytes was measured by counting RECA-1 and PDGFR- $\beta$  double-positive cells at D21. The number of Msi-1–positive neural stem cells was measured by counting Msi-1 and TOPRO-3 double-positive cells at D21.

### **Brain Atrophy Evaluation**

To assess brain atrophy and infarct volume at D21, six coronal sections taken at 0.6mm intervals between the levels of 1.6 mm rostral and 1.4 mm caudal to the bregma were stained with Cresyl violet. Ipsilateral ventricle size was calculated by multiplying the sum of the areas by the distance between sections using WinRoof software. Volumes of intact tissue in ipsilateral ischemic and contralateral normal side of the brain were also calculated by multiplying the sum of the areas by the distance between sections using WinRoof software. Infarct volume was indirectly measured by subtracting the volume of intact tissue in the ipsilateral hemisphere from that of the contralateral hemisphere.<sup>23</sup> In this study, infarct volume was not corrected for brain swelling because brain swelling had resolved by D21.<sup>24</sup>

### **Trophic and Chemotactic Factor Analysis**

Rats were divided into three groups at 24 h post-stroke: young hMSC group (24-year-old MSCs  $1 \times 10^6$  cells/300  $\mu$ l, n=4); old hMSC group (64-year-old MSCs  $1 \times 10^6$  cells/300  $\mu$ l, n=4); and control group (PBS 300  $\mu$ l, n=4). At D7, rats were anaesthetised and euthanised. Rat brains were removed after perfusion with cold saline via the ascending aorta, and small pieces were cut from the peri-infarct cortex. Then, brains were homogenised in PBS as a 10% solution, and cytokine/chemokine levels were measured by Luminex assay and enzyme-linked immunosorbent assay (ELISA) according to the manufacturer's protocol.

A MILLIPLEX MAP kit was used to measure the concentrations of vascular endothelial growth factor (VEGF) and monocyte chemotactic protein-1 (MCP-1). A rat BDNF ELISA Kit (Boster Biological Technology, Pleasanton, CA, USA) was used to measure the concentrations of BDNF.

### **Direction Index Analysis**

As there appeared to be a relationship between the process alignment of GFAP-positive cells and Msi-1-positive neural stem cell migration, the direction of the processes of GFAP-positive cells was analysed. To obtain quantitative information about the tendency of the direction of GFAP-positive cells, image analysis was performed. This analysis

consisted of two steps: simplification of the original picture and quantification of the direction of GFAP-positive cells.

### 1. Simplification of the original image

One of the images is shown as an illustrative example (Figure 1a). Here, colour is expressed by RGB values from 0 to 255, and these values are referred to as  $V_R$ ,  $V_G$ , and  $V_B$ , respectively. First, only red regions (cell region) using the following criteria were selected:

$$\frac{V_R}{V_G} > 2.0, \quad (1)$$

$$\frac{V_R}{V_B} > 2.0, \quad (2)$$

$$V_R > 128. \quad (3)$$

Pixels whose colour satisfied these three criteria were considered to be a red pixel, and the others were considered to be a black pixel. Black pixels were changed into white colour (Figure 1b). Because the image contained large signals connected with each other as well as signals that were too small, it was necessary to simplify them to obtain quantitative information about the direction of GFAP-positive cells. The next step was to divide the large signals connected with each other into small signals. Signals with a size larger than 1.0% of the total size of the image were picked up, and the narrowest position in each signal as a cutting position was determined. By changing the colour of these

cutting positions to white, the large signals could be divided into small signals. This dividing process was repeated until all the signals were smaller than 1.0% of the total size of the image. Finally, the largest 100 signals were picked up, and small signals were deleted. The final image is shown in Figure 1c, which was sufficiently simple for the quantification of GFAP-positive cell direction.

## 2. Quantification of the direction of cells

One signal from 100 signals is shown as an illustrative example (Figure 1d). First, a line perpendicular to the infarct core was drawn, such that the direction to the infarct core was defined (Figure 1d). In this example,  $\theta$  was 42 degrees. Next, a local XY-coordinate system for each signal was introduced. In this coordinate system, the origin was the centre of the mass of the signal, the X-axis was parallel to the direction to the infarct core, and the Y-axis was normal to the X-axis (Figure 1d). Coordinates of all the pixels in the signal were examined, and the average values of X-coordinates,  $\langle x \rangle$ , and Y-coordinates,  $\langle y \rangle$ , were obtained. Using these two average values, a value related to the direction of the signal using the following equation was obtained:

$$V_{dir} = \frac{\langle x \rangle}{\langle y \rangle} - 1.0 . \quad (4)$$

If this value was larger than 0, it was considered that the signal extended toward the X-axis. When this value was negative, the signal extended toward the Y-axis. In this example,

the pixel number was 1280,  $\langle x \rangle$  was 22.11, and  $\langle y \rangle$  was 10.30 (Figure 1e), indicating  $V_{dir}$  was 1.15. This value indicated that this signal extended in the X-axis direction. Thus, the average value of  $V_{dir}$  over all the signals determined the tendency of the direction of the signals. The average value of  $V_{dir}$  was defined as the Direction index. As a result, quantitative information about the tendency of the direction of GFAP-positive cells in the image could be obtained.

### **Statistical Analysis**

Data are presented as the mean  $\pm$  SD or median (interquartile range (IQR), 25–75<sup>th</sup> percentile). The Steel-Dwass test was used to evaluate significant differences between the three groups in mNSS by point. The Mann-Whitney *U*-test or Tukey-Kramer multiple comparison test following one-way ANOVA were used to evaluate all significant differences between two or three groups. Spearman's rank method was used to evaluate significant correlation. Log-rank test with Kaplan-Meier curve was used to evaluate significant differences in survival rate. The text and figure legends describe the statistical tests used. Unless stated differently, all tests were 2-tailed. Differences were considered statistically significant at  $P < 0.05$ .

### **Results**

### **Young hMSCs Secrete High Levels of BDNF**

Analysis of CM by Luminex assay showed that the levels of BDNF and PDGF-BB secreted differed depending on hMSC age, and were negatively correlated with age ( $P=0.044$ ,  $R=-0.63$  and  $P=0.048$ ,  $R=-0.79$ , Spearman, Figure 2a, c). The levels of BDNF were significantly higher in young hMSCs ( $76.27\pm 63.20$  pg/ml/ $10^4$  cells) compared with old hMSCs ( $19.45\pm 15.86$  pg/ml/ $10^4$  cells;  $P=0.017$ , Figure 2b). A similar trend was seen for PDGF-BB, but this was not statistically significant (young hMSCs:  $40.47\pm 11.58$  pg/ml/ $10^4$  cells v. old hMSCs:  $25.35\pm 8.28$  pg/ml/ $10^4$  cells;  $P=0.11$ , Figure 2d). Doubling time was not statistically different between the groups (young hMSCs:  $3.97\pm 1.46$  days v. old hMSCs:  $5.18\pm 1.97$  days;  $P=0.87$ , Supplemental Figure 1).

### **Young hMSCs Provide Better Functional Recovery and Prevent Atrophy**

Body weight before surgery was not statistically different ( $P=0.25$ ) between the groups:  $289.8\pm 10.16$  g in the control group ( $n=10$ ),  $281.5\pm 10.06$  g in the old hMSC group ( $n=8$ ), and  $283\pm 12.81$  g in the young hMSC group ( $n=9$ ). Rats did not show any neurological deficits before surgery (Figure 3a). Intra-arterial delivery of hMSCs significantly enhanced functional recovery as assessed by the mNSS at D14, D17, and D21 (Figure 3a). Interestingly, young hMSCs induced an early recovery at D7, and



provided a marked improvement by D21 (median 4.00 [IQR, 3.00–4.00]) compared with controls (median 6.00 [IQR, 6.00–6.25];  $P=0.0006$ ) or old hMSCs (median 5.00 [IQR, 5.00–6.00];  $P=0.0075$ ). Furthermore, old hMSCs provided significantly better functional recovery at D21 compared with controls ( $P=0.047$ ). Infarct volume and brain atrophy were assessed by Cresyl violet staining at D21 (Figure 3b). There was no statistically significant difference in infarct volume between groups:  $73.97\pm 16.82\text{ mm}^3$  in controls,  $70.39\pm 17.75\text{ mm}^3$  in the old hMSC group and  $69.61\pm 19.78\text{ mm}^3$  in the young hMSC group ( $P=0.86$ , Supplemental Figure 2). However, ipsilateral ventricle size was significantly smaller in the young hMSC group ( $3.47\pm 2.24\text{ mm}^3$ ) compared with controls ( $8.92\pm 5.11\text{ mm}^3$ ;  $P=0.046$ ) or old hMSC group ( $9.29\pm 6.00\text{ mm}^3$ ;  $P=0.044$ , Figure 3c). The survival rate of transplanted hMSCs in the peri-infarct cortex at D2 and D7 was not different between young and old hMSC groups, and no transplanted hMSCs were detected at D21 (Supplemental Figure 3). There was no statistically significant difference ( $P=0.85$ , Figure 3d) in animal survival rate at D21: 81.6% in the young hMSC group ( $n=26$ ), 68.6% in the old hMSC group ( $n=25$ ), and 73.7% in controls ( $n=19$ ).

### **Donor Age Affects Trophic and Chemotactic Factor Secretion at D7**

It is well known that PDGF-BB and BDNF are involved in atherosclerosis, wound healing, angiogenesis, inflammation, and neurogenesis.<sup>25-34</sup> BDNF, MCP-1, and VEGF

play key roles in angiogenesis, inflammation, and neurogenesis after cell transplantation, and PDGF-BB and BDNF have been reported to affect the expression of these factors.<sup>35-</sup>

<sup>37</sup> Therefore, we focused on BDNF, MCP-1, and VEGF expression. The level of BDNF was significantly lower in the control group ( $446.0 \pm 114.3$  pg/ml) than in the old hMSC ( $882.7 \pm 89.46$  pg/ml;  $P=0.0004$ ) and young hMSC groups ( $914.0 \pm 89.53$  pg/ml;  $P=0.0002$ ), but no difference was seen between the old and young hMSC groups (Figure 4a). However, the value of MCP-1 was significantly higher in the young hMSC group ( $0.56 \pm 0.086$  pg/ml) compared with the old hMSC group ( $0.33 \pm 0.084$  pg/ml;  $P=0.005$ , Figure 4b). The levels of VEGF did not differ statistically between the young and old hMSC groups ( $P=0.549$ , Figure 4c).

### **Donor Age Affects Anti-inflammatory Effects and Vessel Maturation at D21**

Intravascular stem cell transplantation affects the host environment by recruiting activated microglia, angiogenesis, and blood-brain barrier (BBB) integrity in the peri-infarct area after stroke.<sup>6, 38</sup> At D21, many Iba-1–positive microglia were present in the peri-infarct cortex (Figure 5a). However, rats receiving hMSCs had fewer Iba-1–positive microglia. The total area of Iba-1–positive microglia in the peri-infarct cortex was significantly lower in the young hMSC group ( $9.30 \pm 5.95\%$ ) than in the controls ( $22.16 \pm 13.17\%$ ;  $P < 0.0001$ ) or the old hMSC group ( $15.29 \pm 14.28\%$ ;  $P=0.032$ ) (Figure

5b).

The area of RECA-1–positive endothelial cells in the peri-infarct cortex was significantly greater in the young hMSC group ( $6.92 \pm 2.28\%$ ) than in the controls ( $5.31 \pm 1.95\%$ ;  $P=0.0001$ ) or the old hMSC group ( $5.30\% \pm 1.80\%$ ;  $P=0.0003$ ) (Figure 6a). Interestingly, the number of RECA-1 and PDGFR- $\beta$  double-positive vessels in the peri-infarct cortex was higher in the young hMSC group ( $113.5 \pm 48.58/\text{mm}^2$ ) than in the controls ( $61.45 \pm 35.89/\text{mm}^2$ ;  $P < 0.0001$ ) or the old hMSC group ( $76.95 \pm 36.94/\text{mm}^2$ ;  $P=0.0003$ ), suggesting that vessel maturation was enhanced by young hMSCs (Figure 6b, c, d).

### **Young hMSCs Enhance Endogenous Neurogenesis with Structural Arrangement**

To assess the relationship between endogenous neural stem cell/progenitor cell migration and astrocytes, the direction of astrocyte processes was examined because GFAP-positive astrocyte processes appeared to stretch toward the infarct core in the young hMSC group compared with the old hMSC group (Figure 7a). The relationship between direction index and the number of Msi-1–positive neural stem cells migrating close to the infarct core was analysed as well as the effect of donor age.

The number of Msi-1–positive neural stem cells migrating close to the infarct core was larger in the young hMSC group ( $1887 \pm 1529/\text{mm}^2$ ) than in the old hMSC group

( $897 \pm 956/\text{mm}^2$ ;  $P=0.0002$ , Figure 7a, b). Interestingly, the direction index in this area positively correlated with the number of Msi-1-positive neural stem cells ( $R=0.2683$ ,  $P=0.0019$ ; Spearman, Figure 7c) and the direction index was significantly larger in the young hMSC group ( $0.377 \pm 0.17$ ) than in the old hMSC group ( $0.278 \pm 0.15$ ;  $P=0.032$ , Figure 7d).

## Discussion

Because the regenerative potential of the body declines with age, even stem cells of the body are prone to the adverse effects of aging.<sup>8</sup> Here we provide evidence that (1) the levels of BDNF and PDGF-BB negatively correlate with age and potentially reduce the capacity for recovery, (2) young hMSCs provide better behavioural recovery by preventing atrophy, (3) the levels of MCP-1 are higher in the peri-infarct cortex treated with young hMSCs than with old hMSCs, (4) anti-inflammatory effects and vessel maturation are enhanced by young hMSCs, and (5) endogenous neural stem/progenitor cell migration positively correlates with astrocyte alignment, which was more pronounced after young hMSC transplantation.

Recently, the accumulation of toxic metabolites, DNA damage, epigenetic alterations, aggregation of damaged proteins, and mitochondrial dysfunctions were reported to be

observed in stem cells from aged donors.<sup>39</sup> Therefore, the numbers of circulating hematopoietic stem cells, endothelial progenitor cells, and MSC are lower in aged individuals, with a decreased proliferative capacity.<sup>40</sup> The expression of various growth factors from MSCs might also be reduced with age.<sup>8, 41</sup> Insulin-like growth factor-1, fibroblast growth factor, VEGF, hepatocyte growth factor, BDNF and nerve growth factor were reported to be higher in young MSCs compared with old MSCs.<sup>8, 41</sup>

Interestingly, it has been reported that the exposure of an aged animal to young blood can counteract and reverse the pre-existing effects of brain aging at the molecular, structural, functional, and cognitive levels.<sup>42</sup> Moreover, Mertens and colleagues compared transcriptomes of human fibroblast induced neurons (iNs) and induced pluripotent stem cells (iPSCs), and found that iNs retained donor aging transcriptomic signatures, while iPSCs were rejuvenated.<sup>43</sup> Taken together, these findings might affect the therapeutic efficacy of stem cell therapy for diseases including stroke, suggesting donor age is one of the critical factors for the success of stem cell treatment.

In our study, there were no differences between young and old hMSCs with regards to the survival rate of transplanted hMSCs, and there were no hMSCs at D21. A previous study reported that although a low number of transplanted hMSCs existed as endothelial cells, the majority of hMSCs had died by D21.<sup>6</sup> However, we found significant

differences in BDNF secretion between young and old hMSCs. Interestingly, the levels of BDNF and PDGF-BB secretion differ depending on hMSC age. BDNF/Tropomyosin-related kinase B signalling enhances the expression of VEGF and the migration of pericytes.<sup>25, 26, 28</sup> PDGF-BB/PDGFR- $\beta$  signalling regulates the regenerative potential and perivascular recruitment of MSCs.<sup>44, 45</sup> Indeed, both PDGFR- $\beta$  and PDGF-BB ligand-null mice die prenatally from haemorrhage and lack pericytes throughout the entire microvascular beds.<sup>46</sup> Moreover, PDGF is a potent inducer of MCP-1, and the PDGF family is closely related to the VEGF family.<sup>47</sup> In this study, we clearly demonstrated that the levels of BDNF and PDGF-BB were negatively correlated with age, following lower MCP-1 levels at D7. Immunohistological analysis also showed better vessel maturation in the peri-infarct cortex of the young hMSC group at D21, possibly induced by BDNF and PDGF-BB. This vessel maturation might enhance BBB integrity. The BBB breakdown caused by less extensive pericyte coverage led to the accumulation of neurotoxins, which contributed to neuroinflammation as represented by increased numbers of activated microglia.<sup>29</sup> Our results are consistent with previous reports showing that donor age negatively affected the immunoregulatory potential of MSCs<sup>9</sup> and that aged bone marrow MSCs increased IL-1 $\beta$ , TNF- $\alpha$ , and IL-6.<sup>48</sup> It was also reported that low levels of serum BDNF were observed in elderly people, and were related to large

white matter hyper-intensity volume with poor visual memory.<sup>49</sup>

During central nervous system development, neurons and precursors migrate into the neocortex along the ascending processes of radial glia.<sup>50, 51</sup> Radial glia were observed in the peri-infarct area adjacent to the core, and these cells stretched their ascending processes in the direction of the infarct core after stroke.<sup>52</sup> When neural stem cells migrate from the subventricular zone to the peri-infarct area, reactive astrocytes guide neural stem cells.<sup>53, 54</sup> Because PDGF-BB, MCP-1, and BDNF were reported to be mediators for proliferation, migration and neurite outgrowth of neuron or neural stem cells,<sup>27, 55, 56</sup> we assessed the interactions between the processes of astrocytes and neural stem cells with regards to donor age. This study is the first to report that astrocyte direction is significantly correlated with the number of neural stem cells, and that the direction index is significantly higher in those receiving young hMSCs compared with old hMSCs. Because young hMSCs secreted higher levels of BDNF *in vitro* and there were higher levels of MCP-1 in the young hMSC group at D7 compared with the old hMSC group, more Msi-1-positive neural stem cells in the young hMSC group migrated close to the infarct core than in the old hMSC group. Thus, multiple trophic factors might be synergistically involved in cell migration.

Cell transplantation therapy was reported to induce angiogenesis by increasing VEGF.<sup>2</sup>

In our study, matured angiogenesis was enhanced in the young hMSC group compared with the old hMSC and control groups. However, there were no differences in the levels of VEGF by analysis of brain homogenates at D7. Vessel formation was increased between D3 and D5, and decreased between D7 and D10 after ischaemic stroke.<sup>57</sup> VEGF was reported to be secreted before vessel formation,<sup>58</sup> and the expression of VEGF was decreased at D7 after cell transplantation following ischaemic stroke.<sup>26, 59</sup> This would affect our result concerning the value of VEGF *in vivo*.

Although the value of MCP-1 was similar between the old hMSC group and control group, the level of BDNF was significantly higher in the old hMSC group compared with the control group at D7, which provided functional recovery at D21. This indicates multiple trophic factors synergistically contribute to functional recovery after cell transplantation following stroke. Finally, the young hMSC group showed better functional recovery with prevention of brain atrophy, which is consistent with clinical findings.<sup>60</sup> The diffuse action of transplanted hMSCs including secretion of multiple trophic factors throughout the brain might affect this. The assessment of brain atrophy might be a factor of functional recovery.<sup>60</sup>

This study had several limitations. First, it was not possible to obtain hMSCs from the same company, because each company had different aged hMSCs. Importantly, all



hMSCs were obtained at passage 2 or 3. To unify the conditions of each hMSC, we used all hMSCs after the next passage with BDNF/PDGF-BB free medium for experiments with the same conditions. Second, the mortality rates of rats were high in our study. The cell dose and occlusion time might affect mortality. Although the dose of hMSCs ( $1 \times 10^6$  cells) injected through the internal carotid artery in our study was not larger compared with other reports,<sup>22, 61, 62</sup> low dose transplantation might reduce the mortality rate. Additionally, limitations in our postoperative animal care might have contributed to the high mortality rate. Future studies will include rehydration therapy for rats with severe stroke. Third, the values of PDGF-BB *in vivo* were not analysed. Fourth, the correlation coefficient between direction index and Msi-1-positive neural stem cells was small possibly because we used two-dimensional, not three-dimensional, analysis. Finally, in our study, the upper age cut-off in the young hMSC group might be lower compared with the donor age in clinical trials. This point should be taken into consideration for clinical translation studies.

In conclusion, donor age of hMSC drastically affects functional and structural outcomes resulting in differences of anti-inflammation, mature angiogenesis, and endogenous neural stem/progenitor cell migration in stroke, possibly by decreased trophic factor secretion. Thus, donor age might be a critical factor for the success of cell transplant

therapy for stroke in clinical settings. Further investigations are needed to elucidate the molecular mechanism of aging of MSCs, leading to new methods to rejuvenate damaged cells.

### **Sources of funding**

This work was supported in part by a grant-in-aid for Scientific Research to Dr. Yamaguchi (#26861155) and Dr. Horie (#26462165).

### **Acknowledgements**

The authors would like to thank Yukio Kato, Department of Dental and Medical Biochemistry, Institute of Biomedical and Health Science, Hiroshima University, for providing hMSCs, Shuntaro Sato, Clinical Research Center, Nagasaki University Hospital, for helpful comments regarding the biostatistics, and Tonya Bliss and Gary K Steinberg, Department of Neurosurgery, Stanford University for helpful discussions and comments.

### **Authors' contributions**

All authors read and approved the final manuscript. S. Y. drafted and revised the

manuscript, participated in the study concept and design, performed experiments, conducted statistical analyses, and analysed the data. N. H. participated in the study concept, and made a substantial contribution to revising the manuscript, design, and interpreting the data. K. S. participated in study concept and performed experiments. T. I. conducted the statistical analyses, analysed and interpreted the data, and partially drafted the manuscript. T. M., H. M. and Y. F. participated in the study concept and performed experiments. S. I., T. H., Y. M., and T. I. participated in the study concept and interpreted the data. N. N. participated in the study concept, made a substantial contribution to revising the manuscript. T. M. participated in the study concept and design.

### **Disclosure/Conflict of Interest**

The authors declare no conflict of interest.

### **Supplementary material**

Supplementary material for this paper can be found at

<http://jcbfm.sagepub.com/content/by/supplemental-data>.

### **References**

1. Goyal M, Menon BK, van Zwam WH, et al. Endovascular thrombectomy after large-vessel ischaemic stroke: a meta-analysis of individual patient data from five randomised trials. *Lancet* 2016; 387: 1723-1731.
2. Bliss T, Guzman R, Daadi M, et al. Cell transplantation therapy for stroke. *Stroke* 2007; 38: 817-826.
3. Rosado-de-Castro PH, Pimentel-Coelho PM, da Fonseca LM, et al. The rise of cell therapy trials for stroke: review of published and registered studies. *Stem Cells Dev* 2013; 22: 2095-2111.
4. Fukuda Y, Horie N, Satoh K, et al. Intra-arterial transplantation of low-dose stem cells provides functional recovery without adverse effects after stroke. *Cell Mol Neurobiol* 2015; 35: 399-406.
5. Yang B, Migliati E, Parsha K, et al. Intra-arterial delivery is not superior to intravenous delivery of autologous bone marrow mononuclear cells in acute ischemic stroke. *Stroke* 2013; 44: 3463-3472.
6. Ishizaka S, Horie N, Satoh K, et al. Intra-arterial cell transplantation provides timing-dependent cell distribution and functional recovery after stroke. *Stroke* 2013; 44: 720-726.
7. Dimmeler S and Vasa-Nicotera M. Aging of progenitor cells: limitation for regenerative capacity? *J Am Coll Cardiol* 2003; 42: 2081-2082.
8. Khan M, Mohsin S, Khan SN, et al. Repair of senescent myocardium by mesenchymal stem cells is dependent on the age of donor mice. *J Cell Mol Med* 2011; 15: 1515-1527.
9. Wu LW, Wang YL, Christensen JM, et al. Donor age negatively affects the immunoregulatory properties of both adipose and bone marrow derived mesenchymal stem cells. *Transpl Immunol* 2014; 30: 122-127.
10. Liu Y, Liu T, Han J, et al. Advanced age impairs cardioprotective function of mesenchymal stem cell transplantation from patients to myocardially infarcted rats. *Cardiology* 2014; 128: 209-219.
11. De Barros S, Dehez S, Arnaud E, et al. Aging-related decrease of human ASC angiogenic potential is reversed by hypoxia preconditioning through ROS production. *Mol Ther* 2013; 21: 399-408.
12. Zhuo Y, Li SH, Chen MS, et al. Aging impairs the angiogenic response to ischemic injury and the activity of implanted cells: combined consequences for cell therapy in older recipients. *J Thorac Cardiovasc Surg* 2010; 139: 1286-1294, 1294 e1281-1282.

13. Yang HC, Rossini M, Ma LJ, et al. Cells derived from young bone marrow alleviate renal aging. *J Am Soc Nephrol* 2011; 22: 2028-2036.
14. Zhang J, Mu X, Breker DA, et al. Atorvastatin treatment is associated with increased BDNF level and improved functional recovery after atherothrombotic stroke. *Int J Neurosci* 2017; 127: 92-97.
15. Kurozumi K, Nakamura K, Tamiya T, et al. Mesenchymal stem cells that produce neurotrophic factors reduce ischemic damage in the rat middle cerebral artery occlusion model. *Mol Ther* 2005; 11: 96-104.
16. De Luca A, Gallo M, Aldinucci D, et al. Role of the EGFR ligand/receptor system in the secretion of angiogenic factors in mesenchymal stem cells. *J Cell Physiol* 2011; 226: 2131-2138.
17. Dufourcq P, Descamps B, Tojais NF, et al. Secreted frizzled-related protein-1 enhances mesenchymal stem cell function in angiogenesis and contributes to neovessel maturation. *Stem Cells* 2008; 26: 2991-3001.
18. Moniche F, Montaner J, Gonzalez-Marcos JR, et al. Intra-arterial bone marrow mononuclear cell transplantation correlates with GM-CSF, PDGF-BB, and MMP-2 serum levels in stroke patients: results from a clinical trial. *Cell Transplant* 2014; 23 Suppl 1: S57-64.
19. Encarnacion A, Horie N, Keren-Gill H, et al. Long-term behavioral assessment of function in an experimental model for ischemic stroke. *J Neurosci Methods* 2011; 196: 247-257.
20. Chen J, Sanberg PR, Li Y, et al. Intravenous administration of human umbilical cord blood reduces behavioral deficits after stroke in rats. *Stroke* 2001; 32: 2682-2688.
21. Tsutsumi S, Shimazu A, Miyazaki K, et al. Retention of multilineage differentiation potential of mesenchymal cells during proliferation in response to FGF. *Biochem Biophys Res Commun* 2001; 288: 413-419.
22. Toyoshima A, Yasuhara T, Kameda M, et al. Intra-Arterial Transplantation of Allogeneic Mesenchymal Stem Cells Mounts Neuroprotective Effects in a Transient Ischemic Stroke Model in Rats: Analyses of Therapeutic Time Window and Its Mechanisms. *PLoS One* 2015; 10: e0127302.
23. Tsuchiya D, Hong S, Kayama T, et al. Effect of suture size and carotid clip application upon blood flow and infarct volume after permanent and temporary middle cerebral artery occlusion in mice. *Brain Res* 2003; 970: 131-139.
24. Argibay B, Trekker J, Himmelreich U, et al. Intraarterial route increases the risk of cerebral lesions after mesenchymal cell administration in animal model of ischemia. *Sci Rep* 2017; 7: 40758. 2017/01/17.

25. Nakamura K, Martin KC, Jackson JK, et al. Brain-derived neurotrophic factor activation of TrkB induces vascular endothelial growth factor expression via hypoxia-inducible factor-1alpha in neuroblastoma cells. *Cancer Res* 2006; 66: 4249-4255.
26. Li N, Wang P, Ma XL, et al. Effect of bone marrow stromal cell transplantation on neurologic function and expression of VEGF in rats with focal cerebral ischemia. *Mol Med Rep* 2014; 10: 2299-2305.
27. Young KM, Merson TD, Sotthibundhu A, et al. p75 neurotrophin receptor expression defines a population of BDNF-responsive neurogenic precursor cells. *J Neurosci* 2007; 27: 5146-5155.
28. Anastasia A, Deinhardt K, Wang S, et al. Trkb signaling in pericytes is required for cardiac microvessel stabilization. *PLoS One* 2014; 9: e87406.
29. Bell RD, Winkler EA, Sagare AP, et al. Pericytes control key neurovascular functions and neuronal phenotype in the adult brain and during brain aging. *Neuron* 2010; 68: 409-427.
30. Chen W, Guo Y, Walker EJ, et al. Reduced mural cell coverage and impaired vessel integrity after angiogenic stimulation in the Alk1-deficient brain. *Arterioscler Thromb Vasc Biol* 2013; 33: 305-310.
31. Sato H, Ishii Y, Yamamoto S, et al. PDGFR-beta Plays a Key Role in the Ectopic Migration of Neuroblasts in Cerebral Stroke. *Stem Cells* 2016; 34: 685-698.
32. Hirschi KK, Rohovsky SA, Beck LH, et al. Endothelial cells modulate the proliferation of mural cell precursors via platelet-derived growth factor-BB and heterotypic cell contact. *Circ Res* 1999; 84: 298-305.
33. Yao Q, Renault MA, Chapouly C, et al. Sonic hedgehog mediates a novel pathway of PDGF-BB-dependent vessel maturation. *Blood* 2014; 123: 2429-2437.
34. Song S, Ewald AJ, Stallcup W, et al. PDGFRbeta+ perivascular progenitor cells in tumours regulate pericyte differentiation and vascular survival. *Nat Cell Biol* 2005; 7: 870-879.
35. Kwon YK. Expression of brain-derived neurotrophic factor mRNA stimulated by basic fibroblast growth factor and platelet-derived growth factor in rat hippocampal cell line. *Mol Cells* 1997; 7: 320-325.
36. Matei D, Kelich S, Cao L, et al. PDGF BB induces VEGF secretion in ovarian cancer. *Cancer Biol Ther* 2007; 6: 1951-1959.
37. Marumo T, Schini-Kerth VB, Fisslthaler B, et al. Platelet-derived growth factor-stimulated superoxide anion production modulates activation of transcription factor NF-kappaB and expression of monocyte chemoattractant protein 1 in human aortic smooth muscle cells. *Circulation* 1997; 96: 2361-2367.

38. Horie N, Pereira MP, Niizuma K, et al. Transplanted stem cell-secreted vascular endothelial growth factor effects poststroke recovery, inflammation, and vascular repair. *Stem Cells* 2011; 29: 274-285.
39. Oh J, Lee YD and Wagers AJ. Stem cell aging: mechanisms, regulators and therapeutic opportunities. *Nat Med* 2014; 20: 870-880.
40. Thijssen DH, Vos JB, Verseyden C, et al. Haematopoietic stem cells and endothelial progenitor cells in healthy men: effect of aging and training. *Aging Cell* 2006; 5: 495-503.
41. Chiba Y, Kuroda S, Osanai T, et al. Impact of ageing on biological features of bone marrow stromal cells (BMSC) in cell transplantation therapy for CNS disorders: functional enhancement by granulocyte-colony stimulating factor (G-CSF). *Neuropathology* 2012; 32: 139-148.
42. Villeda SA, Plambeck KE, Middeldorp J, et al. Young blood reverses age-related impairments in cognitive function and synaptic plasticity in mice. *Nat Med* 2014; 20: 659-663.
43. Mertens J, Paquola AC, Ku M, et al. Directly Reprogrammed Human Neurons Retain Aging-Associated Transcriptomic Signatures and Reveal Age-Related Nucleocytoplasmic Defects. *Cell Stem Cell* 2015; 17: 705-718.
44. Lin RZ, Moreno-Luna R, Li D, et al. Human endothelial colony-forming cells serve as trophic mediators for mesenchymal stem cell engraftment via paracrine signaling. *Proc Natl Acad Sci U S A* 2014; 111: 10137-10142.
45. Folkman J and D'Amore PA. Blood vessel formation: what is its molecular basis? *Cell* 1996; 87: 1153-1155.
46. Lindahl P, Johansson BR, Leveen P, et al. Pericyte loss and microaneurysm formation in PDGF-B-deficient mice. *Science* 1997; 277: 242-245.
47. Bethel-Brown C, Yao H, Hu G, et al. Platelet-derived growth factor (PDGF)-BB-mediated induction of monocyte chemoattractant protein 1 in human astrocytes: implications for HIV-associated neuroinflammation. *J Neuroinflammation* 2012; 9: 262.
48. Bustos ML, Huleihel L, Kapetanaki MG, et al. Aging mesenchymal stem cells fail to protect because of impaired migration and antiinflammatory response. *Am J Respir Crit Care Med* 2014; 189: 787-798.
49. Pikula A, Beiser AS, Chen TC, et al. Serum brain-derived neurotrophic factor and vascular endothelial growth factor levels are associated with risk of stroke and vascular brain injury: Framingham Study. *Stroke* 2013; 44: 2768-2775.
50. Noctor SC, Flint AC, Weissman TA, et al. Neurons derived from radial glial cells establish radial units in neocortex. *Nature* 2001; 409: 714-720.
51. Rakic P. Mode of cell migration to the superficial layers of fetal monkey neocortex.

*J Comp Neurol* 1972; 145: 61-83.

52. Shimada IS, Peterson BM and Spees JL. Isolation of locally derived stem/progenitor cells from the peri-infarct area that do not migrate from the lateral ventricle after cortical stroke. *Stroke* 2010; 41: e552-560.
53. Saha B, Peron S, Murray K, et al. Cortical lesion stimulates adult subventricular zone neural progenitor cell proliferation and migration to the site of injury. *Stem Cell Res* 2013; 11: 965-977.
54. Jin K, Sun Y, Xie L, et al. Directed migration of neuronal precursors into the ischemic cerebral cortex and striatum. *Mol Cell Neurosci* 2003; 24: 171-189.
55. Widera D, Holtkamp W, Entschladen F, et al. MCP-1 induces migration of adult neural stem cells. *Eur J Cell Biol* 2004; 83: 381-387.
56. Bianchi LM, Daruwalla Z, Roth TM, et al. Immortalized mouse inner ear cell lines demonstrate a role for chemokines in promoting the growth of developing statoacoustic ganglion neurons. *J Assoc Res Otolaryngol* 2005; 6: 355-367.
57. Wei L, Erinjeri JP, Rovainen CM, et al. Collateral growth and angiogenesis around cortical stroke. *Stroke* 2001; 32: 2179-2184.
58. Yancopoulos GD, Davis S, Gale NW, et al. Vascular-specific growth factors and blood vessel formation. *Nature* 2000; 407: 242-248.
59. Wakabayashi K, Nagai A, Sheikh AM, et al. Transplantation of human mesenchymal stem cells promotes functional improvement and increased expression of neurotrophic factors in a rat focal cerebral ischemia model. *J Neurosci Res* 2010; 88: 1017-1025.
60. Bang OY, Lee JS, Lee PH, et al. Autologous mesenchymal stem cell transplantation in stroke patients. *Ann Neurol* 2005; 57: 874-882.
61. Janowski M, Lyczek A, Engels C, et al. Cell size and velocity of injection are major determinants of the safety of intracarotid stem cell transplantation. *J Cereb Blood Flow Metab* 2013; 33: 921-927.
62. Mitkari B, Nitzsche F, Kerkela E, et al. Human bone marrow mesenchymal stem/stromal cells produce efficient localization in the brain and enhanced angiogenesis after intra-arterial delivery in rats with cerebral ischemia, but this is not translated to behavioral recovery. *Behav Brain Res* 2014; 259: 50-59.



## Figure legends

### Figure 1: Direction index analysis.

(a) An original image to illustrate the direction index analysis. (b) An image of the first step of simplification, where black pixels were changed into white colour. (c) An image of the second step of simplification, where large signals were divided into small signals and excessively small signals were deleted, resulting in 100 signals remaining. (d) Direction to the infarct core was defined (in this case,  $\theta$  is 42 degrees). (e) A local coordinate system was introduced for each signal, and average X- and Y-coordinate values for all pixels in the signal were calculated.

### Figure 2: Analysis of conditioned medium by Luminex assay *in vitro*.

(a) The level of brain-derived neurotrophic factor (BDNF) was negatively correlated with donor age ( $R=-0.63$  and  $P<0.05$ , Spearman). (b) The level of BDNF was significantly higher in young human mesenchymal stem cells (hMSCs) ( $n=5$ ) compared with old hMSCs ( $n=6$ ) (Mann-Whitney  $U$ -test, \*  $P<0.05$ ). (c) The level of platelet-derived growth factor (PDGF-BB) was negatively correlated with donor age ( $R=-0.79$  and  $P<0.05$ , Spearman). (d) There were no differences in the levels of PDGF-BB between young hMSCs ( $n=3$ ) and old hMSCs ( $n=4$ ). All data are presented as mean  $\pm$  SD.

**Figure 3:** Assessment of outcomes and brain atrophy with Cresyl violet staining after treatment.

(a) Rats treated with young human mesenchymal stem cells (hMSCs) (n=9) showed better behavioural recovery by modified neurological severity score than controls (n=10) or old hMSCs (n=8) (Steel-Dwass test, \*  $P < 0.05$  vs Control, #  $P < 0.05$  vs Old hMSC). Each point represents the median (interquartile range, 25–75<sup>th</sup> percentile) in the graph. (b) Cresyl violet staining. Scale bar = 1 mm. (c) Left ventricle size in young hMSCs was significantly smaller than controls or old hMSCs (one-way ANOVA, Tukey-Kramer multiple comparison test, \*  $P < 0.05$ ). Data are presented as mean  $\pm$  SD. (d) There were no significant differences in animal survival rates between the three groups (n=26 in young hMSC group, n=25 in old hMSC group and n=19 in controls; Log-rank test).

**Figure 4:** Analysis of trophic and chemotactic factors in the peri-infarct cortex at D7.

(a) Analysis of brain homogenates from the peri-infarct cortex by enzyme-linked immunosorbent assay at D7. The level of brain-derived neurotrophic factor (BDNF) was higher in young (n=4) and old human mesenchymal stem cell (hMSC) groups (n=4) compared with controls (n=4). (b), (c). Analysis of brain homogenates from the peri-infarct cortex by Luminex assay at D7. The levels of monocyte chemoattractant protein-1

(MCP-1) in young hMSCs were significantly higher than in old hMSCs. There were no significant differences in the level of vascular endothelial growth factor (VEGF) between the three groups (one-way ANOVA, Tukey-Kramer multiple comparison test, \*  $P < 0.05$ ).

Data are presented as mean  $\pm$  SD.

**Figure 5:** Analysis of anti-inflammatory effects in the peri-infarct cortex at D21.

(a), (b) Immunohistochemical staining at the peri-infarct cortex showed that the Iba-1-positive area in the young human mesenchymal stem cell (hMSC) group was significantly smaller than in controls or the old hMSC group (one-way ANOVA, Tukey-Kramer multiple comparison test, \*  $P < 0.05$ , \*\*  $P < 0.01$ ). Data are presented as mean  $\pm$  SD. Scale bar = 50  $\mu\text{m}$ .

**Figure 6:** Analysis of angiogenesis in the peri-infarct cortex at D21.

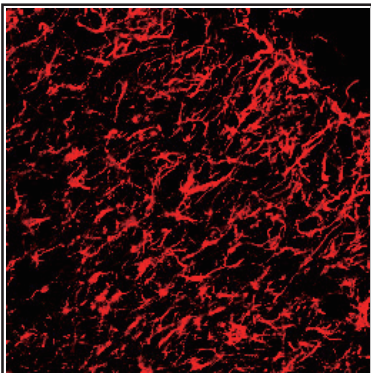
(a) Immunohistochemical staining at the peri-infarct cortex showed that the RECA-1-positive area in the young human mesenchymal stem cell (hMSC) group was significantly larger than in controls or the old hMSC group. (b) The number of platelet-derived growth factor receptor (PDGFR)- $\beta$ -positive vessels in the young hMSC group was higher than in controls or the old hMSC group (one-way ANOVA, Tukey-Kramer multiple

comparison test, \*\*  $P < 0.01$ ). (c), (d) RECA-1 and PDGFR- $\beta$  double staining images at the peri-infarct cortex. Data are presented as mean  $\pm$  SD. Scale bar = 50  $\mu\text{m}$ , (c), 10  $\mu\text{m}$  (d), magnified image.

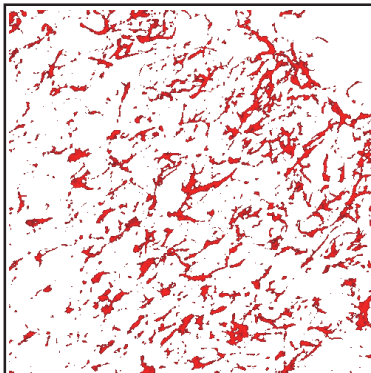
**Figure 7:** Analysis of neurogenesis in peri-infarct cortex at D21.

(a) Glial fibrillary acidic protein (GFAP) and Musashi-1 (Msi-1) double staining. Scale bar = 50  $\mu\text{m}$ . IC: infarct core. (b) The number of Msi-1-positive neural stem cells at the peri-infarct cortex at D21 was significantly larger in the young human mesenchymal stem cells (hMSC) group than in controls and the old hMSC group (one-way ANOVA, Tukey-Kramer multiple comparison test, \*\*  $P < 0.01$ ). (c) The direction index was significantly correlated with the number of Msi-1-positive cells migrating close to the infarct core ( $R = 0.2683$  and  $P < 0.01$ , Spearman). (d) The direction index of the young hMSC group was significantly higher than in the old hMSC group (one-way ANOVA, Tukey-Kramer multiple comparison test, \*  $P < 0.05$ ). Data are presented as mean  $\pm$  SD.

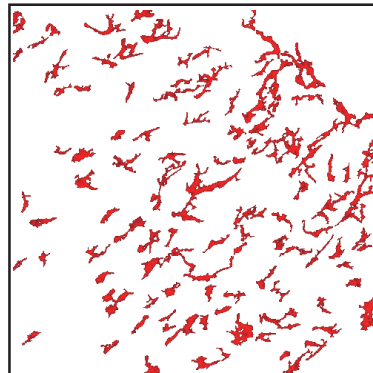
(a)



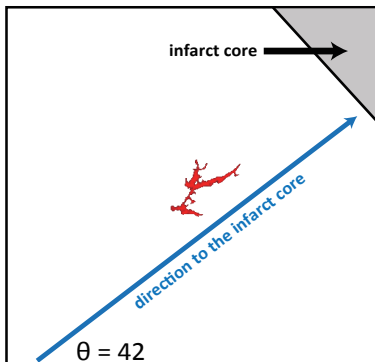
(b)



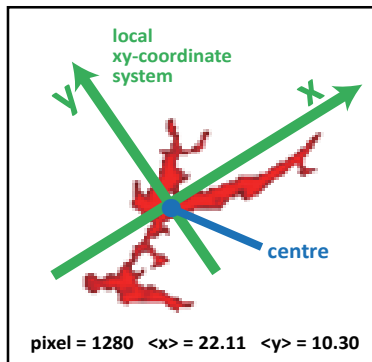
(c)



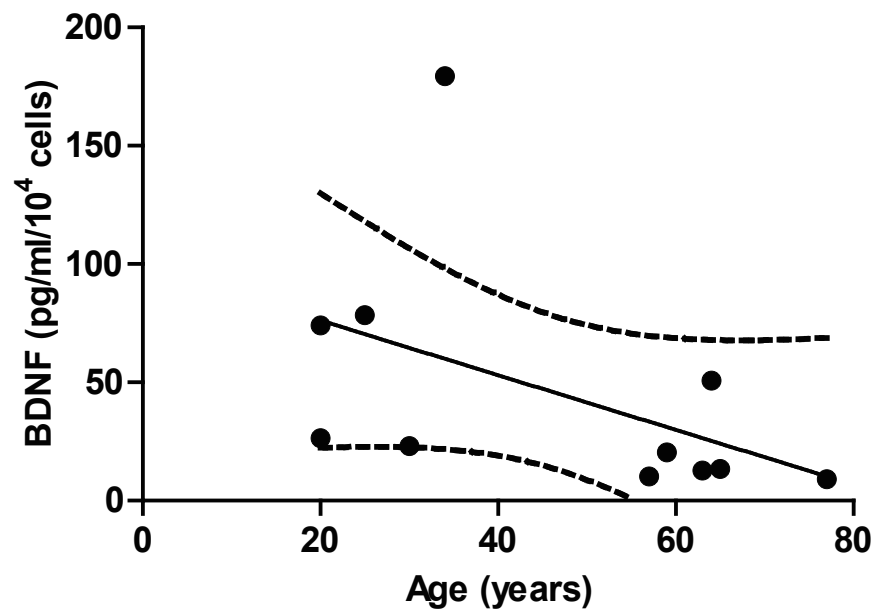
(d)



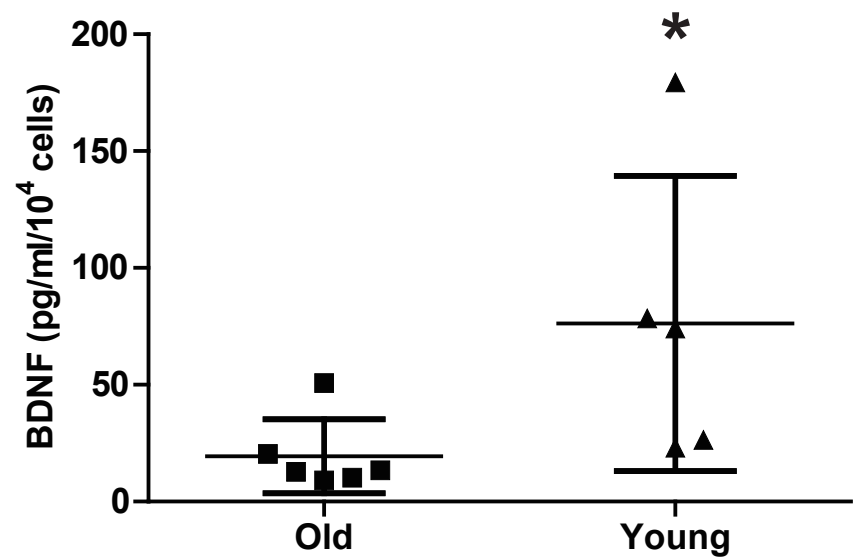
(e)



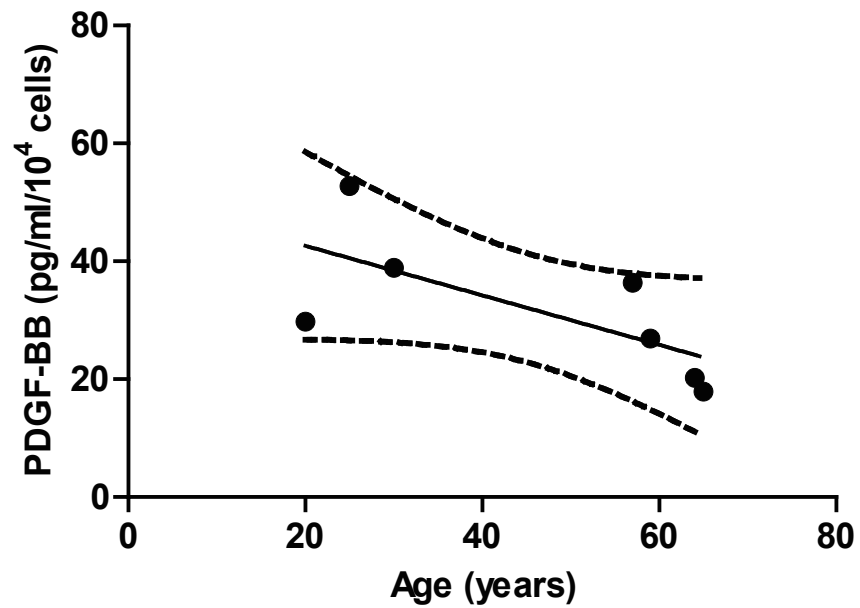
(a)



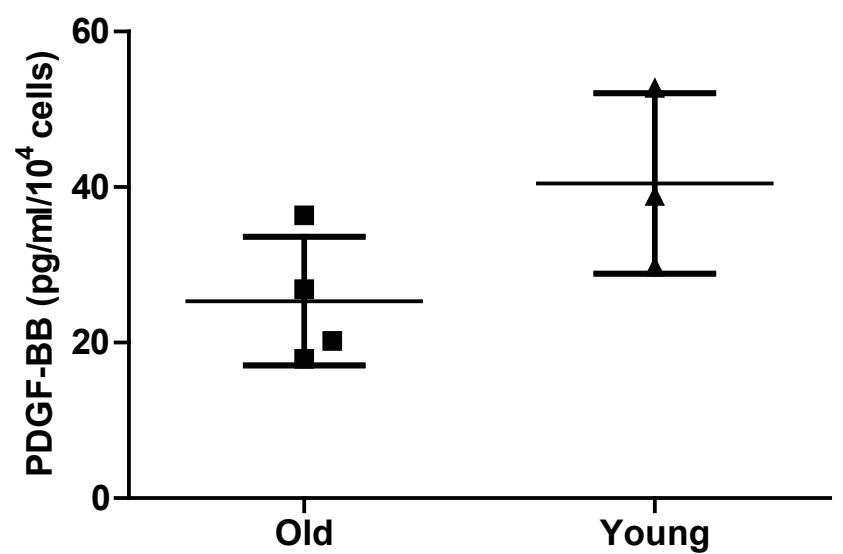
(b)



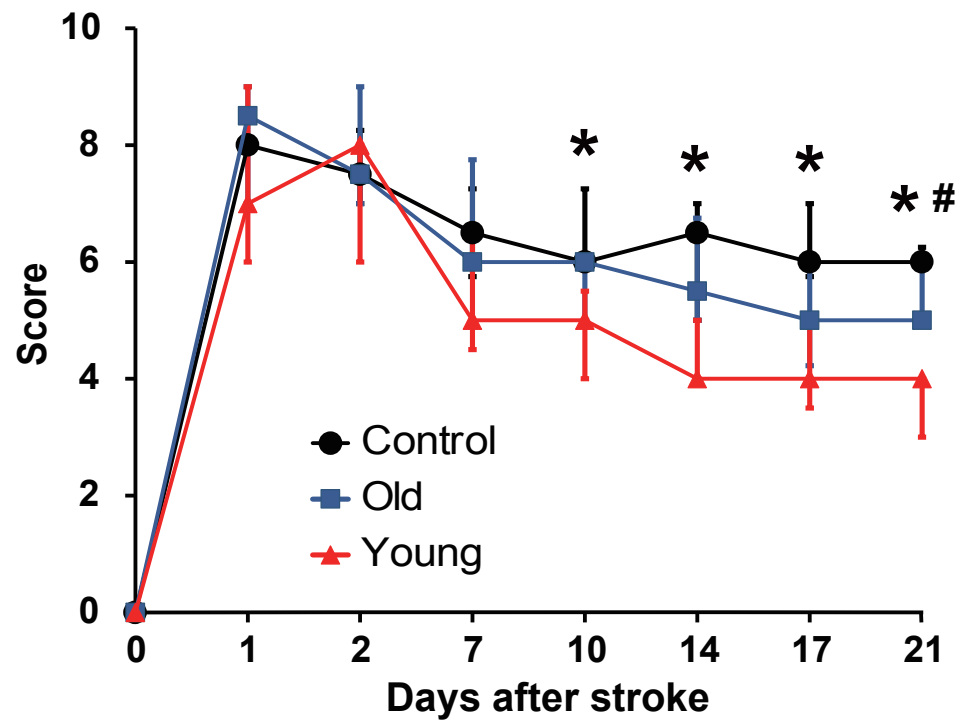
(c)



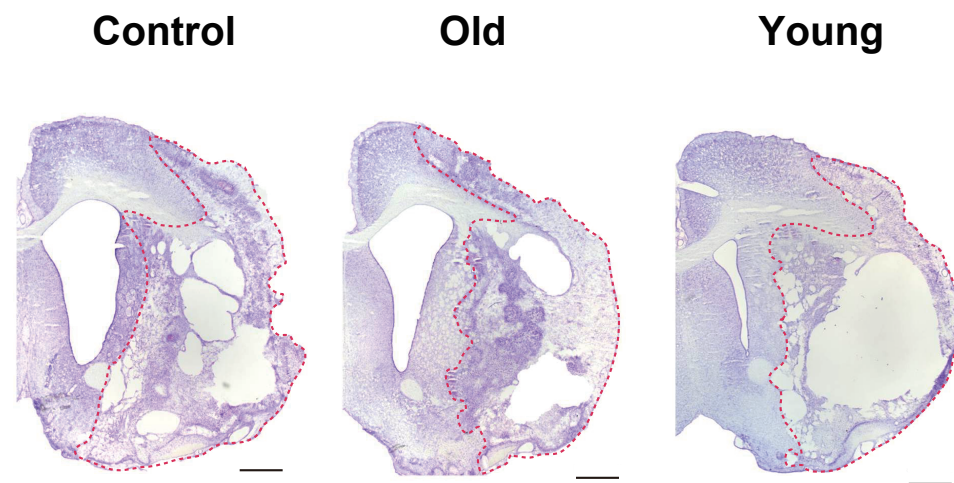
(d)



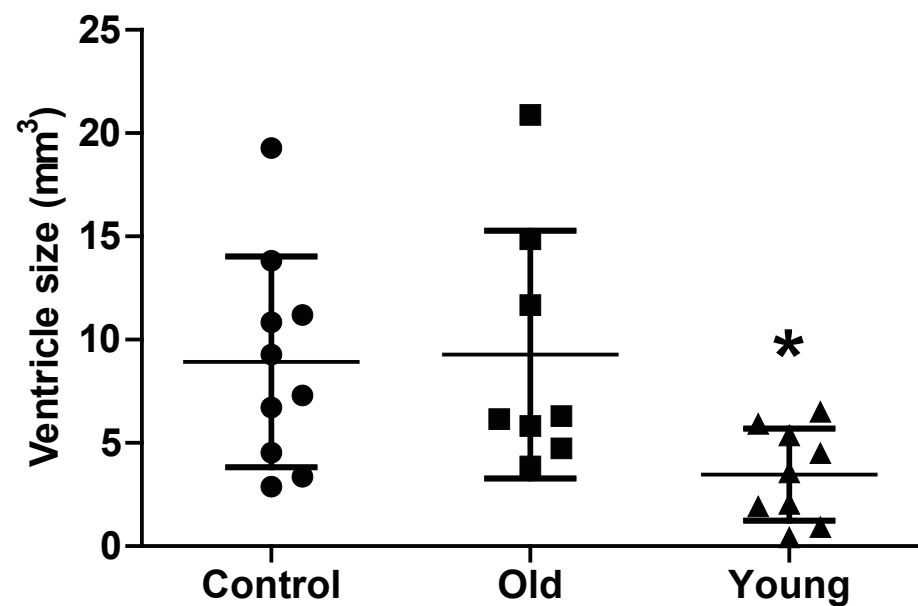
(a)



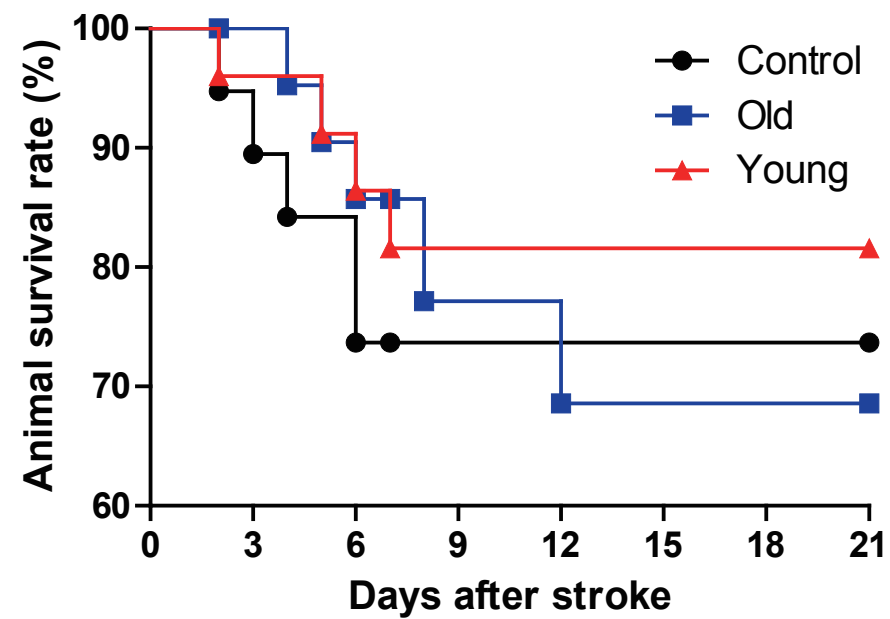
(b)



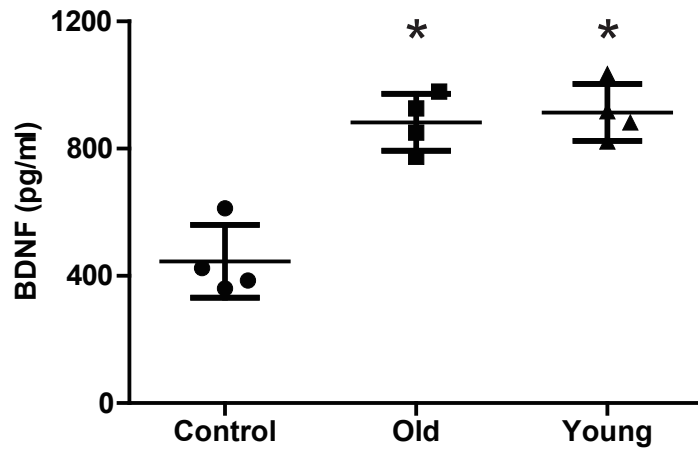
(c)



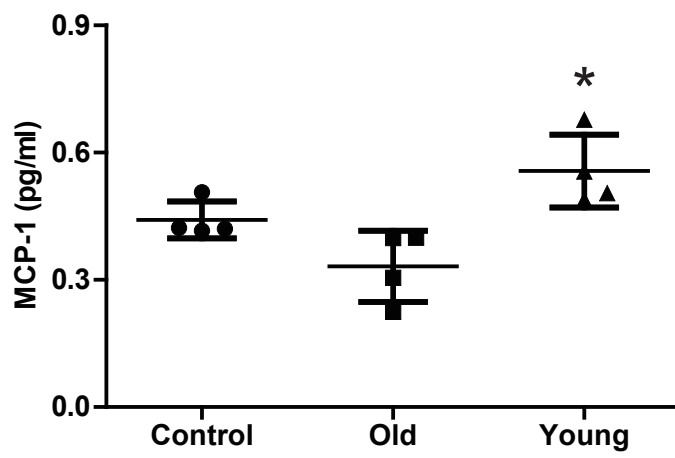
(d)



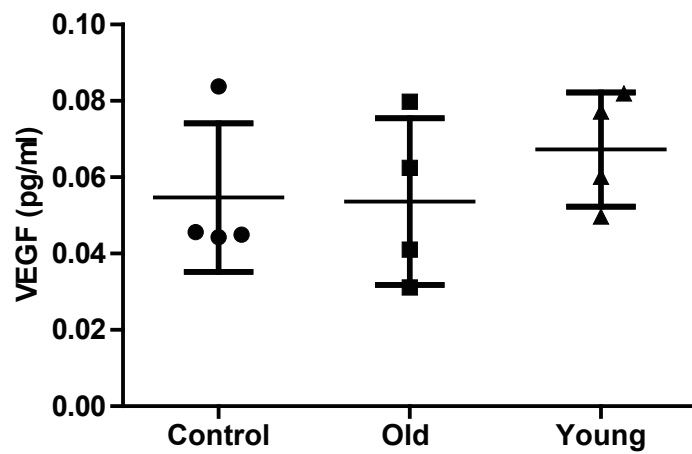
(a)



(b)

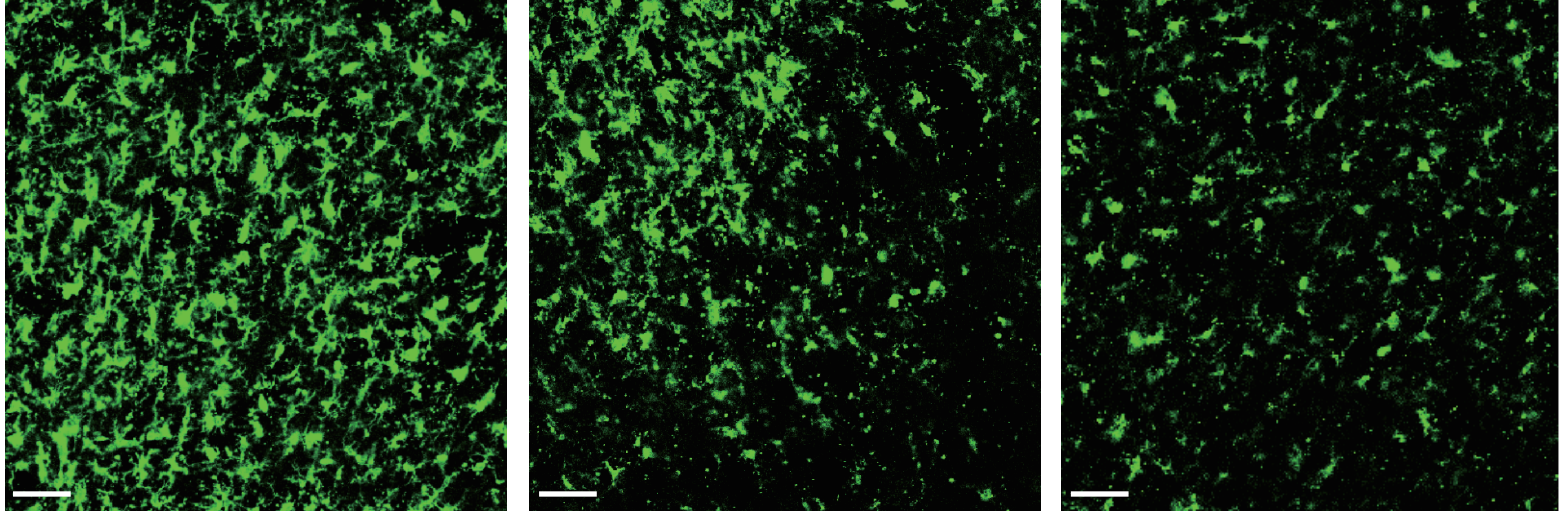


(c)

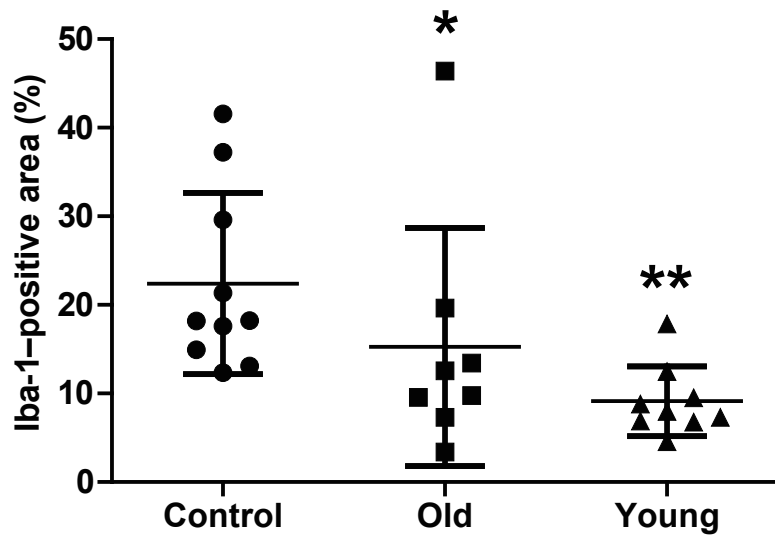


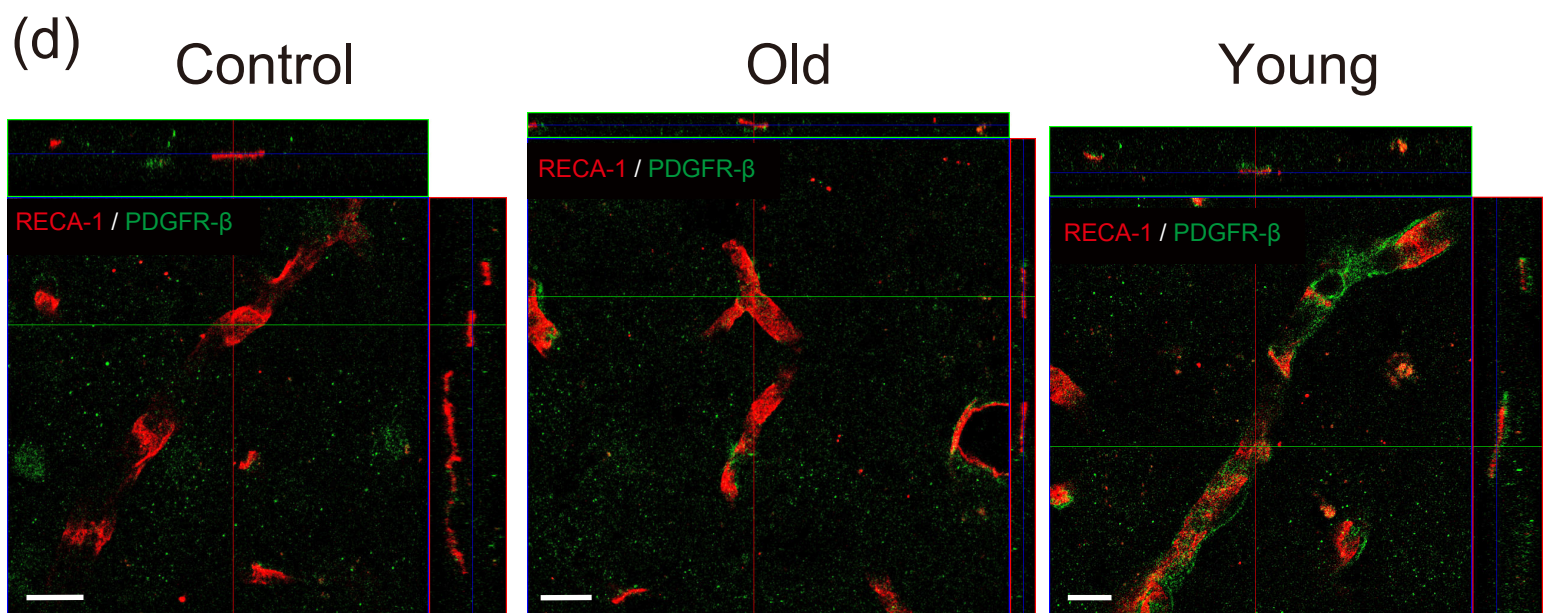
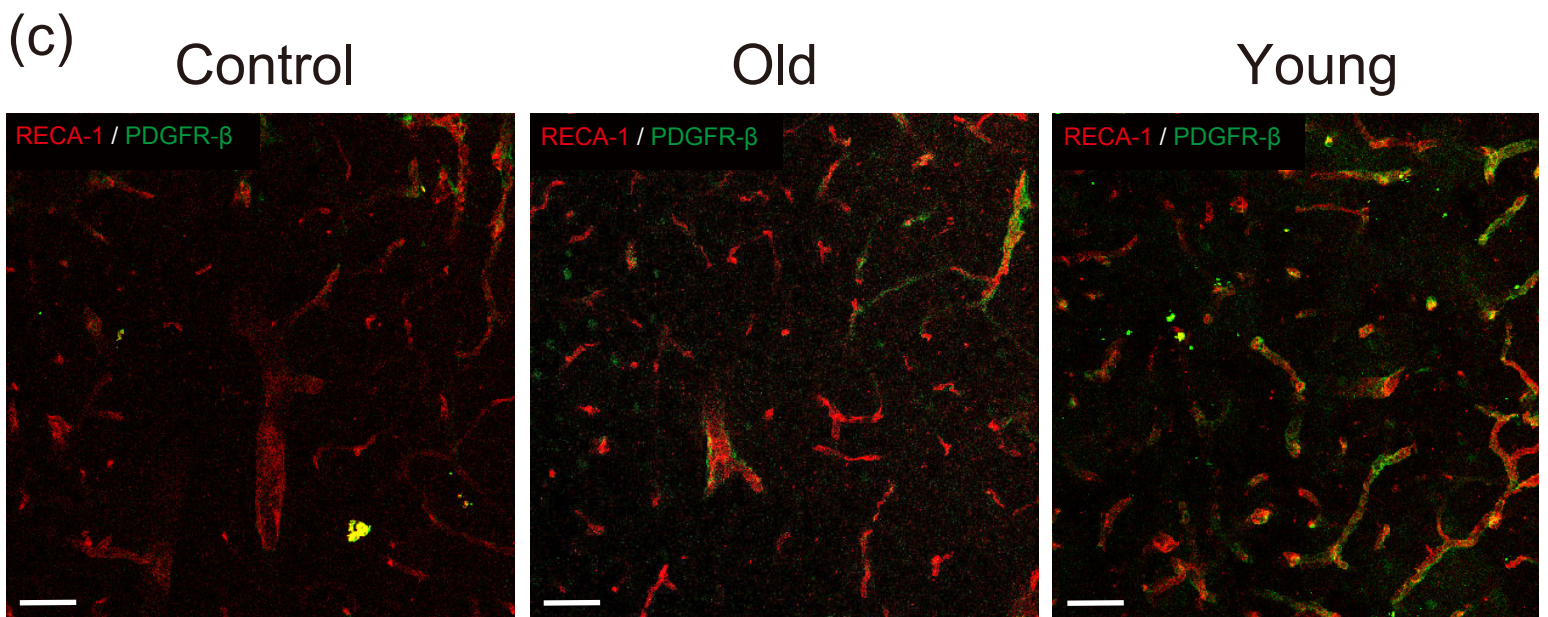
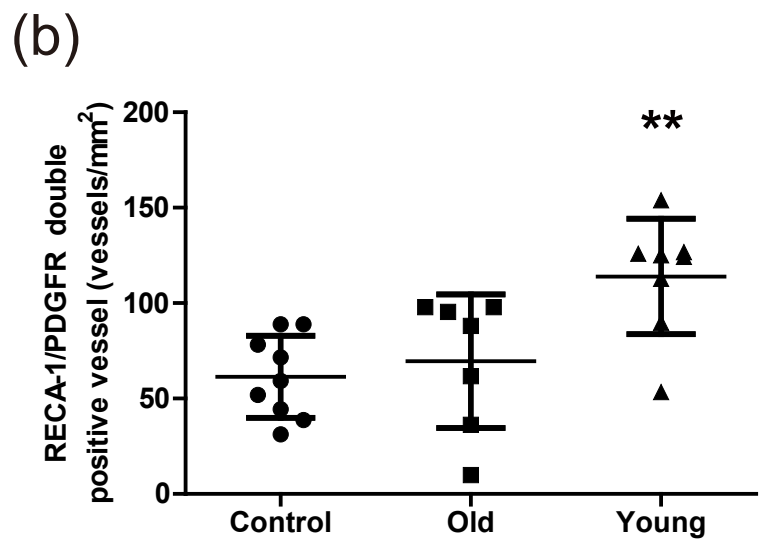
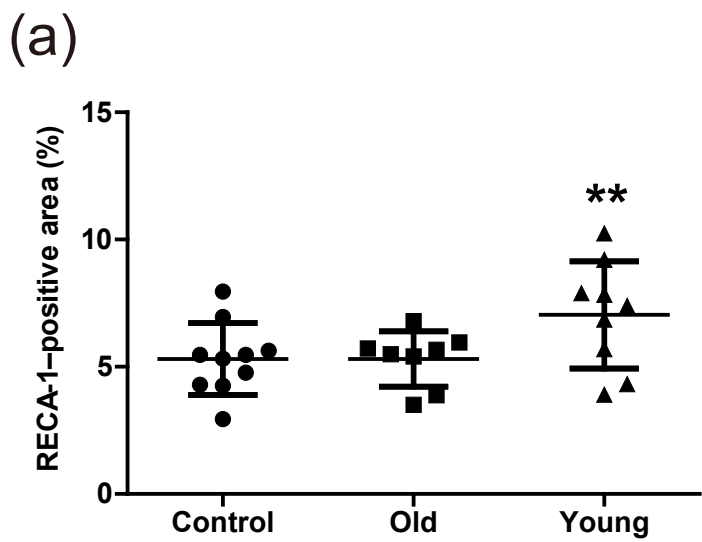


(a) Control Old Young

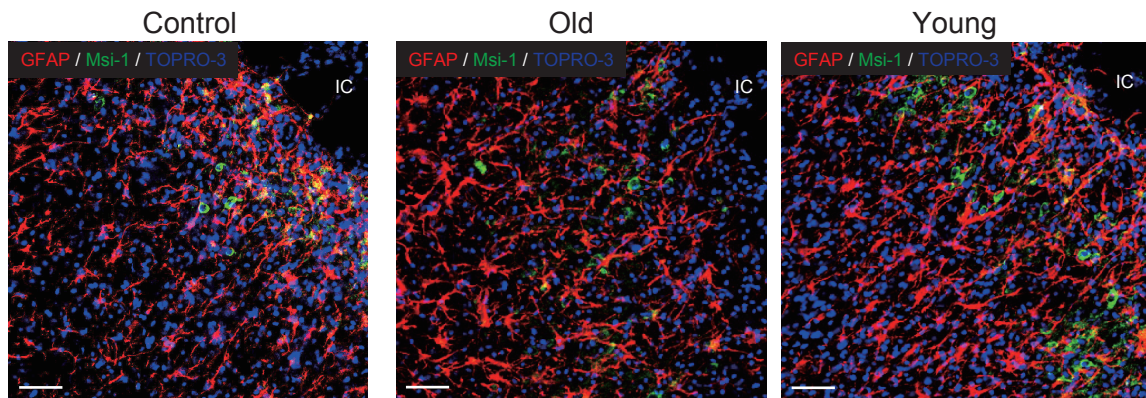


(b)

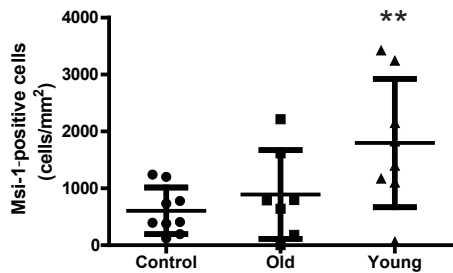




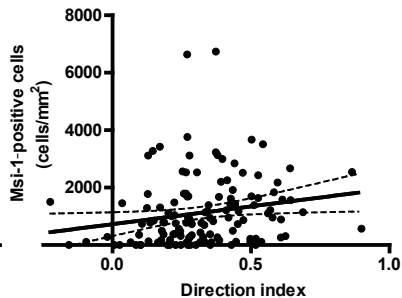
(a)



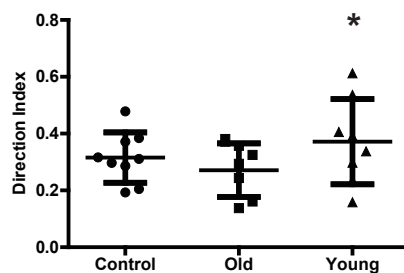
(b)



(c)



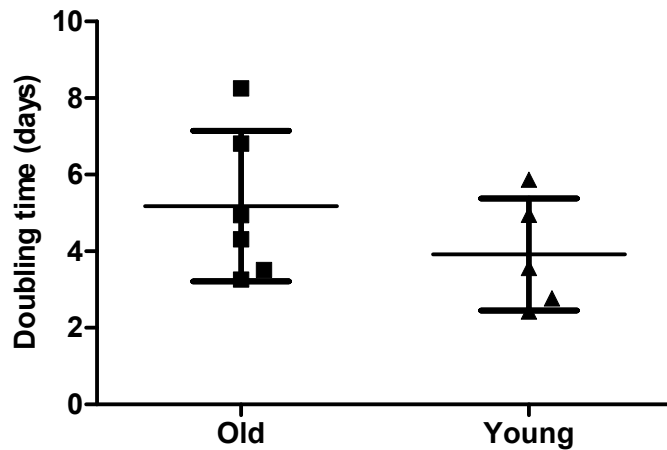
(d)



## Supplemental material

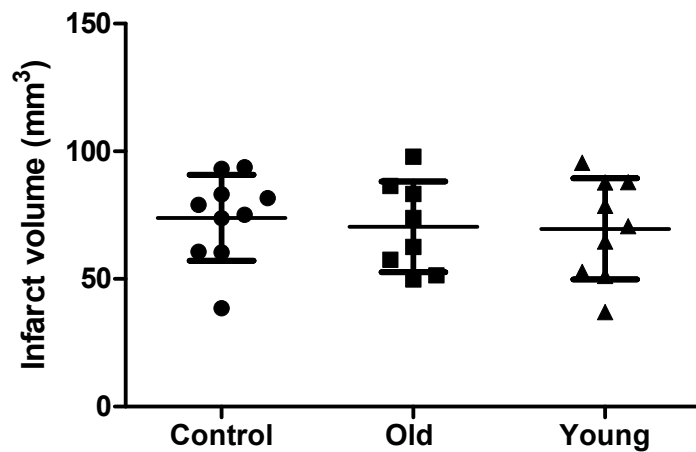
### Supplemental Figure 1

There were no significant differences in doubling time between the young and old hMSCs.



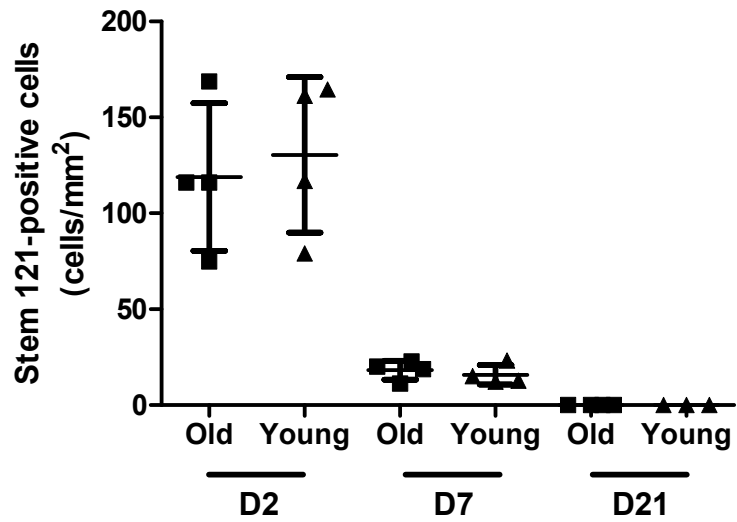
### Supplemental Figure 2

There were no significant differences in infarct volume between the three groups at D21.



### Supplemental Figure 3

There were no significant differences in the number of STEM 121-positive hMSCs between the old (n=4) and young hMSC (n=4) groups at the peri-infarct cortex at D2 and D7. Stem 121 positive hMSCs were not observed at D21 in both groups.



### Supplementary Table 1

Rats with cerebral infarction	Total number	
1) Eligible mNSS from 6 to 9 points at 24 h post-stroke	70	
2) Ineligible mNSS outside 6 to 9 points at 24 h post-stroke	16	
Total number of rats	86	
Control group	Total number	Death number
1) Functional examination and histological analysis at D21	12	2
2) Analysis of trophic and chemotactic factors by Luminex and ELISA	7	3
Total number of rats	19	5
Old hMSC group	Total number	Death number
1) Functional examination and histological analysis at D21	12	4
2) Analysis of trophic and chemotactic factors by Luminex and ELISA	4	0
3) Immunohistochemistry for Stem 121 at D2 and D7	9	1
Total number of rats	25	5
Young hMSC group	Total number	Death number
1) Functional examination and histological analysis at D21	11	2
Exclusion due to postoperative cervical hematoma	1	
2) Analysis of trophic and chemotactic factors by Luminex and ELISA	4	0
3) Immunohistochemistry for Stem 121 at D2 and D7	10	2
Total number of rats	26	4

hMSC, human mesenchymal stem cells; mNSS, modified Neurological Severity Score; ELISA, enzyme-linked immunosorbent assay

## Supplementary Table 2

### Modified Neurological Severity Score Points

---

Motor tests	
Raising rat by tail	3
Flexion of forelimb	1
Flexion of hindlimb	1
Head moved > 10° to vertical axis within 30 s	1
Placing rat on floor (normal=0; maximum=3)	3
Normal walk	0
Inability to walk straight	1
Circling toward paretic side	2
Falls down to paretic side	3
Sensory tests	2
Placing test (visual and tactile test)	1
Proprioceptive test (deep sensation, pushing paw against table edge to stimulate limb muscles)	1
Beam balance tests (normal=0; maximum=6)	6
Balances with steady posture	0
Grasps side of beam	1
Hugs beam and 1 limb falls down from beam	2
Hugs beam and 2 limb fall down from beam, or spins on beam (>60 s)	3
Attempts to balance on beam but falls off (>40 s)	4
Attempts to balance on beam but falls off (>20 s)	5
Falls off; no attempt to balance or hang on to beam (<20 s)	6
Reflex absence and abnormal movements	4
Pinna reflex (head shake when auditory meatus is touched)	1
Corneal reflex (eye blink when cornea is lightly touched with cotton)	1
Startle reflex (motor response to a brief noise from snapping a clipboard paper)	1
Seizures, myoclonus, myodystony	1
Maximum points	18

---

One point is awarded for inability to perform the tasks or for lack of a tested reflex: 13-18, severe injury; 7-12, moderate injury; 1-6, mild injury.

(Reference)

Chen J, Sanberg PR, Li Y, et al. Intravenous administration of human umbilical cord blood reduces behavioral deficits after stroke in rats. *Stroke*. 2001; 32: 2682-8.